Chapter 5

Excitation-Intensity (EI) Effect on Photoluminescence of ZnO Materials with Various Morphologies

Prasada Rao Talakonda

Additional information is available at the end of the chapter

http://dx.doi.org/10.5772/64937

Abstract

The chapter discusses about excitation-intensity effects on photoluminescence emission peaks of zinc oxide (ZnO) material. ZnO is an ideal material for optoelectronic devices due to its wide band gap of 3.37 eV and some exciting optical properties. The performance of optoelectronic devices is greatly affected by the vibrational properties of the material, which are influenced by the interaction of phonons with free and bound electron-hole pairs. The photoluminescence (PL) spectroscopy is used to understand the extrinsic and intrinsic defects in ZnO materials. Understanding PL of ZnO nanostructures/thin films may lead to development of more efficient ZnO-based optoelectronic devices.

Keywords: ZnO, Defects, excitation intensity, photoluminescence

1. Introduction

Luminescence is one of the fastest growing and most useful analytical techniques in science and technology. The applications of luminescence can be found in various subject areas as materials science, microelectronics, clinical chemistry, biology, physics, environmental science, chemistry, toxicology, biochemistry, pharmaceuticals, and medicine. The term luminescence includes a wide variety of light-emitting processes, which originate their names from the varied sources of excitation energy that power them.

Photoluminescence (PL) spectroscopy is a sensitive nondestructive technique, suitable for identifying point defects including extrinsic and intrinsic defects in materials [1]. It is a useful tool to evaluate the quality and to study the physical parameters of semiconductor materials

in the form of thin films and nanomaterials. Zinc oxide (ZnO) is one of the promising semiconductor materials of II–VI group, because of its wider band gap (3.37 eV) and large excitation binding energy (60 meV) at room temperature [2]. ZnO thin films and nanostructures are increasingly being used in light-emitting diodes, solar cells, chemical sensors, photocatalysis, and antibacterial materials, etc., because of their unique physical properties [2, 3].

In general, defects and impurities are playing an important role in the semiconductor industry to develop devices. In the case of ZnO material, it is very difficult to understand and study the role of defects or impurities in order to develop optoelectronic devices. Native or intrinsic defects are existing in the ZnO material such as oxygen vacancies (V_O), zinc interstitials (Zn_i), oxygen interstitial (O_i), zinc vacancies (V_{Zn}), zinc antisites, and oxygen antisites. Understanding the incorporation and behavior of intrinsic defects in ZnO material is essential to its successful application in optoelectronic devices. These native defects have long been believed to play an important role in ZnO-based devices. The band-to-band excitation of ZnO promotes electrons from the valence band to the conduction band, leaving holes in the valence band. The holes migrate from the valence band to deep levels and recombination occurs between electrons from either the conduction band or shallow donor levels and trapped holes on deep levels [4–6]. Basically, the PL of ZnO is related to the presence of holes in the valence band [4]. The PL spectroscopy can help to understand the extrinsic and intrinsic defects in ZnO materials. Understanding of PL on ZnO nanostructure/thin films may lead to development of more efficient ZnO-based optoelectronic devices.

The PL properties of ZnO materials have been widely studied by many research groups and several research groups noticed that excitation intensity (EI) also has important influence on the PL spectra of ZnO material [7, 8]. The current chapter is providing more details about the EI effects on ZnO materials with different morphologies. Three different sets of ZnO samples were deposited on various substrates with three kinds of morphologies. PL and Raman spectra were recorded using LABRAM-HR spectrometer excited with a 325 nm He-Cd laser at room temperature. The excitation intensity-dependent PL and Raman spectra were obtained at room temperature by changing the laser intensity with the change of optical filters. The laser intensity was fixed as P_0 for without filter (no filter). The EI for different filters denoted as $D_{0.03} = P_0/2$, $D_{0.06} = P_0/4$, $D_1 = P_0/10$, $D_2 = P_0/100$, $D_3 = P_0/1000$, $D_4 = P_0/10{,}000$. Low-temperature PL and Raman spectra were obtained using WITec instrument. The crystal structure and morphology of the samples were characterized by X-ray diffraction (XRD) and scanning electron microscopy (SEM).

2. Results

2.1. ZnO thin films

ZnO thin films with thickness of 450 nm were deposited on glass substrates using spray pyrolysis (SP) technique. The precursor solution for spray pyrolysis was prepared by dissolving appropriate amounts of zinc acetate dihydrate in a mixture of deionized water and ethanol at room temperature. In this mixture, ethanol concentration was 10 ml in 100 ml solution. A

http://dx.doi.org/10.5772/64937

solution of 0.3 M Zn $(CH_3CO_2)_2$ was used as a precursor, prepared by the dissolving in deionized water and ethanol [3]. A few drops of acetic acid were added to aqueous solutions to prevent the formation of hydroxides. ZnO thin films were deposited on glass substrates at a substrate temperature of 623 K. The glass substrates were cleaned thoroughly with acetone, isopropanol, deionized water, and finally cleaned with the help of an ultrasonic bath for 30 min and dried [3, 9]. The spray nozzle was at a distance of 20 cm from the substrate during deposition [3, 9]. The solution flow rate was held constant at 3 ml/min. Air was used as the carrier gas at the pressure of 2 bar [3, 9]. The structural and morphological properties of ZnO thin films are shown in **Figure 1**.

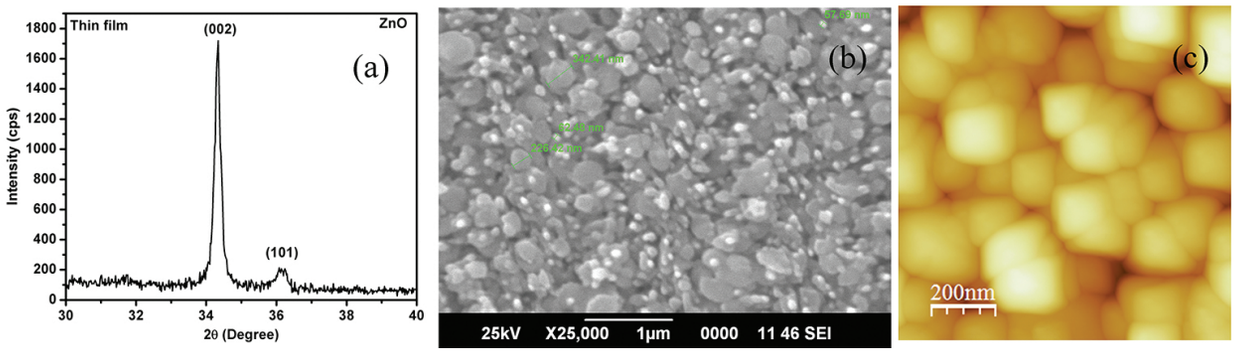

Figure 1. (a) XRD, (b) SEM, and (c) AFM.

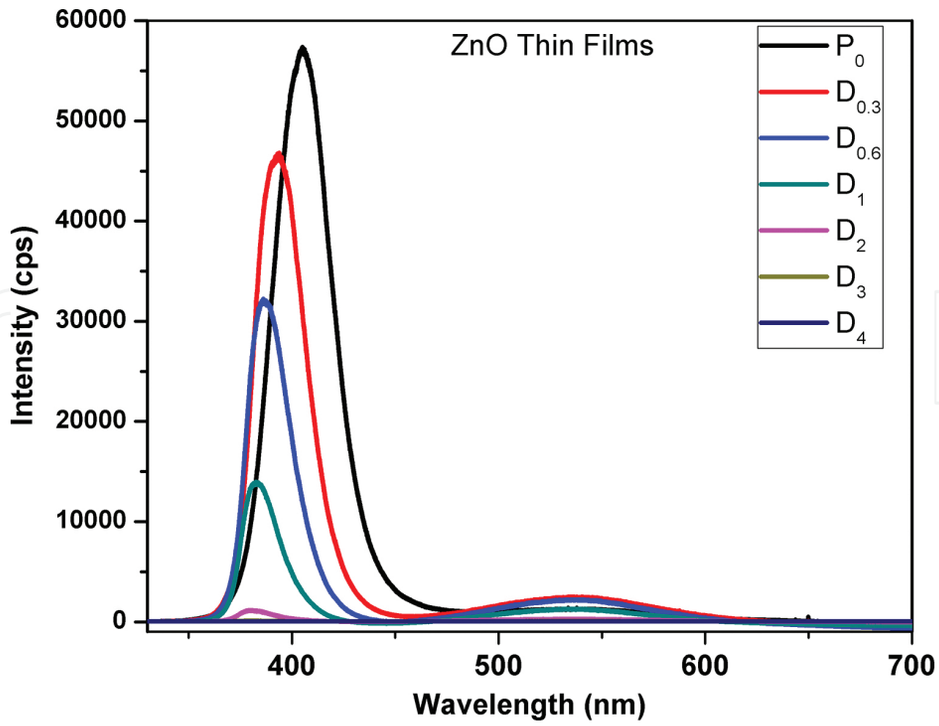

Figure 2. PL emission peak intensity variation with EI intensity.

The XRD studies have shown that all the diffraction peaks belong to ZnO wurtzite structure and the (0 0 2) diffraction peak related to the *c*-axes is predominant. No other phase was observed. The ZnO thin films are having uniform grains on the surface. These grains are uniformly distributed on the surface of the films without any voids. This can be understood from the SEM and AFM studies (**Figure 1**). The room temperature PL studies are shown in **Figure 2**.

The PL spectrum of ZnO thin films consists of two major emission peaks: a sharp peak located at ultraviolet region, and a weak broad peak in the visible region. According to the previous reports, the appearance of UV emission and visible emission indicates that the existence of native defects in ZnO. The intensity of UV peak of ZnO thin films is decreases with the decreasing EI. The UV emission peak position moved toward lower wavelength side (406–380 nm) with the decreasing of EI. The UV emission peak variation with EI could not explained completely by previous reports. Some previous reports were explained this kind of effect using the concept of laser-induced heating effect. The EI variation studies have extend for different ZnO samples with different morphology (nanorods, tetrapods, etc.) to understand EI effect on ZnO material.

2.2. ZnO nanorods

Nanorods structures like ZnO material were deposited on ITO substrate by electrochemical deposition (EC) technique. Electrolytes were zinc nitrate hydrate ($Zn(NO_3)_2{\cdot}6H_2O$) and analytic-grade hexamethylenetetramine ($C_6H_{12}N_4$). **Figure 3** shows XRD and the FESEM images of rod-like ZnO nanostructures with different magnifications that have been grown on ITO substrate. The nanostructures are arbitrarily directed and a nonuniform distribution of dense, arbitrarily directed ZnO nanorods, and no branching is observed, which indicates that the ZnO nanorods are grown from spontaneous nucleation.

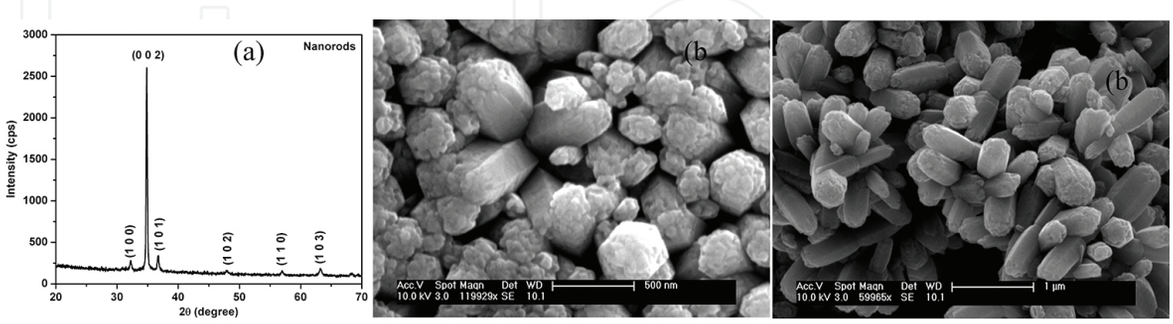

Figure 3. (a) XRD and (b) SEM.

Figure 4 shows that the PL spectrum of ZnO nanorods. The UV emission peak position exhibits a significant blue-shift from 417 to 377 nm with a range of about 40 nm with decrease of EI. The UV peak intensity also varied with the EI.

http://dx.doi.org/10.5772/64937

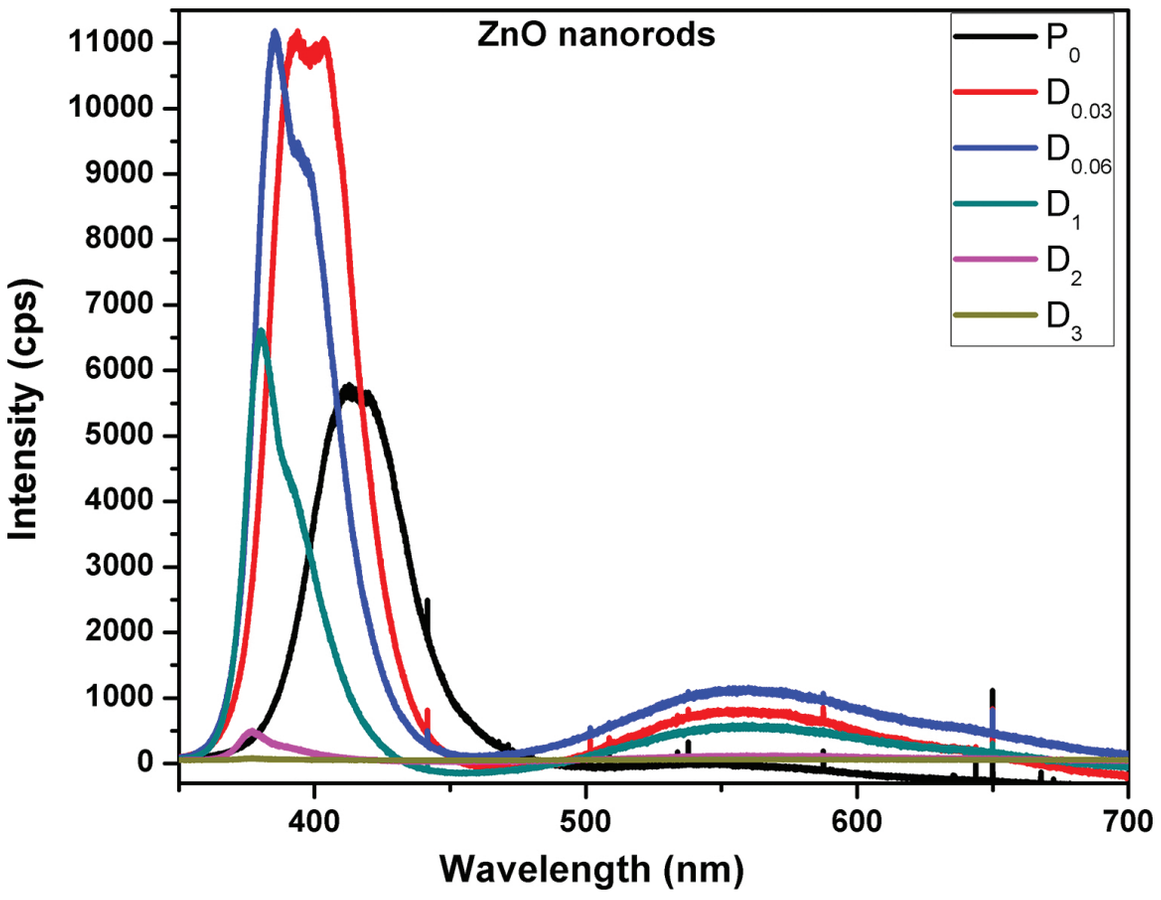

Figure 4. PL spectrum of ZnO nanorods.

2.3. ZnO tetrapods

ZnO tetrapods were synthesized on silicon substrate by vaporizing Zn granule (99.8% purity) in a quartz tube of 30 mm diameter and 100 cm in length at 1200°C in a horizontal tube furnace for 30 min duration at a heating rate of 10°C/min in ambient. **Figure 5** shows the XRD and SEM of ZnO tetrapods.

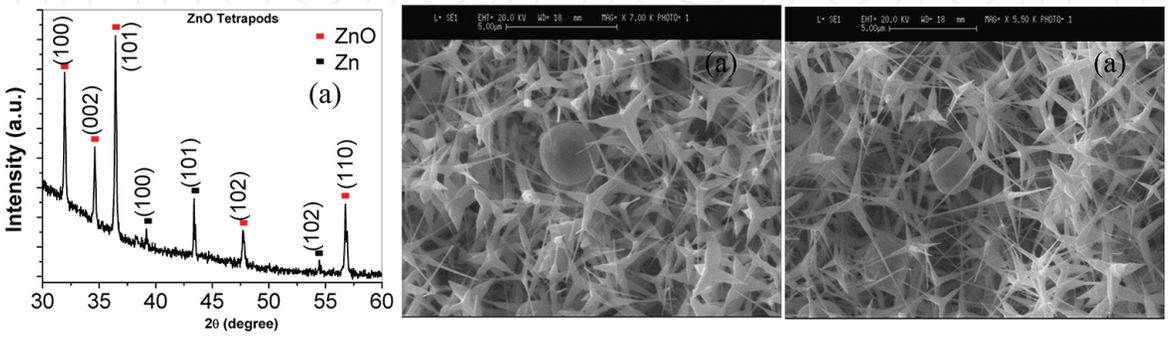

Figure 5. ZnO tetrapods (a) XRD and (b) SEM.

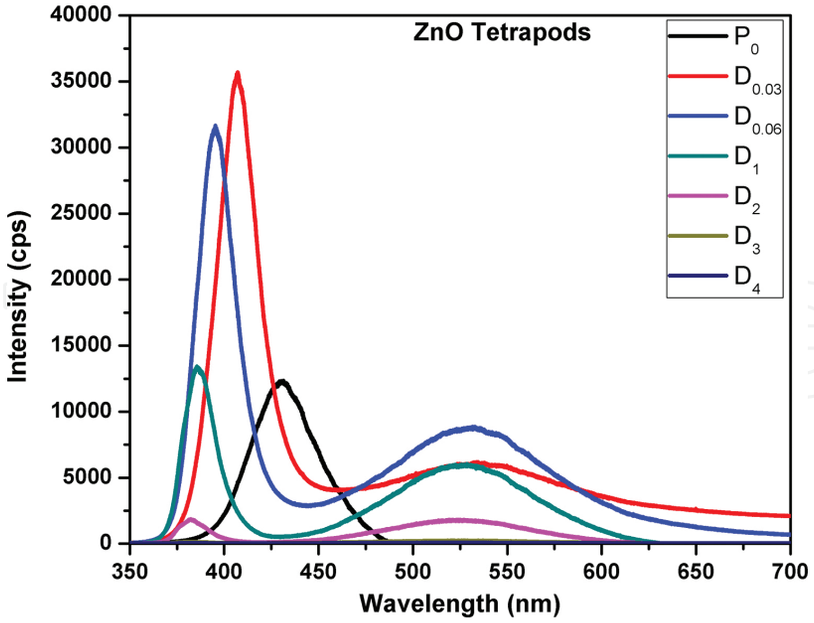

Figure 6. PL spectrum of ZnO tetrapods.

The PL spectrum of ZnO tetrapods is shown in **Figure 6**. The UV emission peak position of ZnO tetrapods moved significantly toward lower wavelength side (from 430 to 380 nm) with the range of about 50 nm when the EI intensity decreased from P_0 to D_4. The intensity of UV peak is increase with EI ranging from P_0 to $D_{0.06}$, and reaches highest at $D_{0.06}$. Then the UV peak intensity decreases and reaches lowest for the D_4.

2.4. ZnO bulk material

Bulk ZnO (ZnO powder) was taken from the Sigma Aldrich for the comparative studies to understand the EI effect on ZnO material. **Figure 7** shows the XRD and SEM of ZnO bulk powder. SEM showed micron-sized particles. The PL spectrum of ZnO bulk material is shown in **Figure 8**. The UV emission peak position and intensity variations are similar to the PL results of ZnO nanorods and ZnO tetrapods.

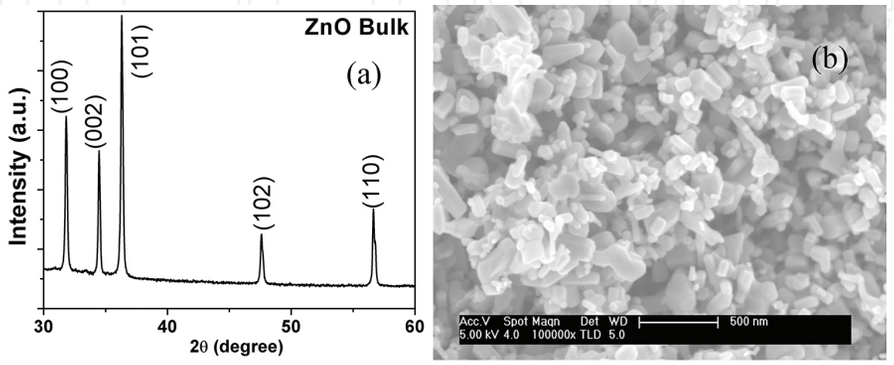

Figure 7. ZnO bulk powder (a) XRD and (b) SEM.

http://dx.doi.org/10.5772/64937

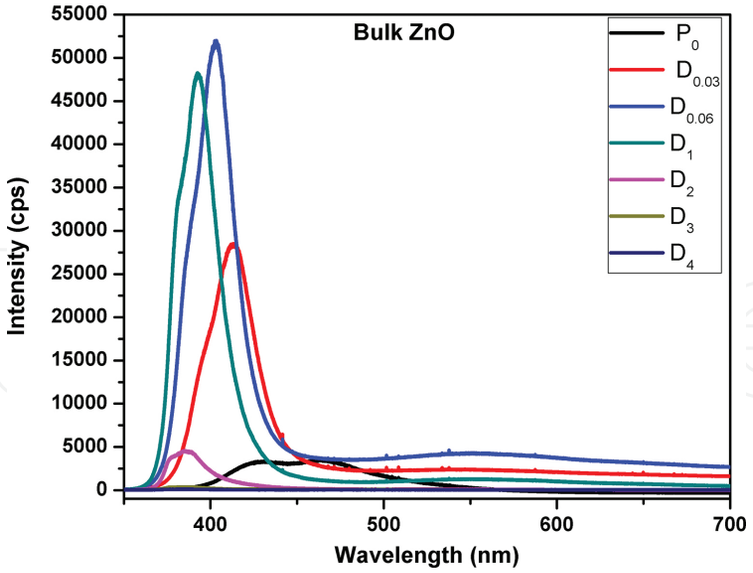

Figure 8. PL spectrum of ZnO bulk powder.

3. Discussion

PL studies show that the UV emission peak position is moved toward higher energy side (blue shift), i.e. lower wavelength side with EI decreases. The blue shift of UV emission peak is observed in all the samples irrespective of their morphology. In the PL spectra of ZnO, recently many research groups are observed that the UV emission peak intensity and peak positions varying with the excitation intensity of laser. In other words, the excitation intensity (EI) strongly influences the PL in ZnO nanostructures including nanocrystals, wires, rods, tetrapods, and ribbons [1, 7, 8, 10]. Hongwei et al. [11] studied the excitation-power dependence of the near-band-edge emission in ZnO inverse opals and nanocrystal films. Zhang et al. [8] studied the effects of excitation intensity (EI) on fluorescence spectra in various ZnO nanostructures, including tetrapod, rod, and sheet-like structures. The EI effects on PL spectra of ZnO nanostructures were explained by many authors using the UV-laser-induced heating effect/laser heating effect. Kurbanov et al. [1] explained UV-laser-induced heating effect using concept of thermal effusivity for ZnO nanocrystals grown on different substrates. In order to understand the local laser heating effects, we have assumed that the laser heating effects increase temperature in the semiconductor material (ZnO nanostructures/thin films). The rising temperature of semiconductor material due localized laser heat effects leads to the changes in optical and vibrational properties of the material [12, 13]. The phonon frequency shifts in ZnO nanostructures/thin films due to laser heating effects can be obtained using Raman spectroscopy. Raman spectroscopy is a nondestructive characterization technique, which is widely used to study the optical and vibrational properties of semiconductor materials including with thin films, hetrostructures, nanocrystals, nanowires, nanoribbons, nanorods, and tetrapods. ZnO is uniaxial crystals with wurtzite structure and it belongs to

$C^4_{(6\vartheta)}(P6_3mc)$ space group. Group theory predicts the existence of the following Raman modes [14]:

$$\Gamma_{opt} = A_1 + 2B_1 + E_1 + 2E_2$$

where Γ is point of the Brillouin zone and it involved in first-order Raman scattering for perfect ZnO crystals. Both A_1 and E_1 modes are polar. They split into transverse optical (A_1TO, E_1TO) and longitudinal optical (A_1LO, E_1LO) modes. E_2 is nonpolar mode consists of two modes of low- and high-frequency phonons (E_2 low, E_2 high). E_2 (high) is associated with oxygen atoms and E_2 (low) is associated with Zn sublattice [13]. These modes are Raman active according to Raman selection rule. B_1 branch is silent. The phonon frequency shifts in the Raman spectra of ZnO nanostructures are probably due to the optical phonon confinement, defects or impurities in the material, tensile strain, and laser-induced heating [13, 14]. The optical phonon confinement effect is neglected in this work because Bohr exciton radii (≈2.34 nm) are smaller than the nanocrystallite size of the grown ZnO nanostructure/thin films.

The PL spectra of ZnO nanostructures with the changes of EI are summarized as follows. In the case of bulk ZnO, the UV peak position moved significantly toward lower wavelength side (from 423.6 to 386.5 nm) with the range of about 37.1 nm when the EI intensity decreased from P_0 to D_4. The intensity of UV peak is increase with EI ranging from P_0 to $D_{0.06}$, and reaches highest at $D_{0.06}$. Then the UV peak intensity decreases and reaches lowest for the D_4. Similar behavior is observed in the case of ZnO nanorods and tetrapods. In the case of ZnO thin films, the intensity of UV peak decreases with the decreasing EI. The green emission peak position is not changed with the EI. The green band intensity is fluctuating with the EI. In other words, the changes in EI not affect by green band position, intensity, and width. Moreover, the appearance of green band in the spectrum is directly supporting the existence of oxygen vacancies or Zn interstitials in the ZnO nanostructure/film. **Figure 9** shows the Raman spectra of ZnO nanostructure/film sample excited using 514 nm laser. The spectrum of bulk ZnO exhibits one prominent peak at 439 cm^{-1} (E_2 high) in addition weak peak at 332 and 579 cm^{-1}. The nanorods also show similar spectrum. In the case of thin films, the prominent peak is observed at 438 cm^{-1} (E_2 high) and weak peaks are observed at 331, 493, and 577 cm^{-1}. The tetrapods of ZnO show prominent peak at 437 cm^{-1} (E_2 high) in addition to weak peaks at 330, 376, and 579 cm^{-1}. In all the cases, the intensity of all the Raman peaks decreases with decreasing EI. The observed values (Raman shift/peak position) are much closed to the previous reports [15, 16]. The Raman peak E_2 high (439/438/437 cm^{-1} representing bulk/rods/tetrapods, respectively) is corresponding to the wurtzite phase of ZnO. The EI variation of the laser (514 nm) does not produce any change in E_2 high peak and other additional peaks position (579/578/577 cm^{-1} representing bulk/rods/tetrapods, respectively). The most important peak is observed at 579/578/577 cm^{-1} in all the ZnO nanostructures. In general, the LO frequency modes are used to observe between 574 and 591 cm^{-1} for the relatively large size of ZnO nanocrystals. According to previous reports [17, 18], the 579/578/577 cm^{-1} mode is ascribed to the LO phonon of A_1 or E_1 symmetry. According to Zhang et al. [14], the peak observed at 577 cm^{-1} is a defect induced

http://dx.doi.org/10.5772/64937

mode in ZnO nanostructures. We believe that the 579/578/577 cm^{-1} corresponding to bulk/rods/tetrapods are defect-induced mode associated with the defects such as oxygen vacancies, zinc interstitials, and the free carrier lack [19]. In the most of the samples (see **Figure 9**), ZnO transversal modes and second order modes are absent in the spectra. This leads to understand poor crystallization quality of ZnO nanostructures.

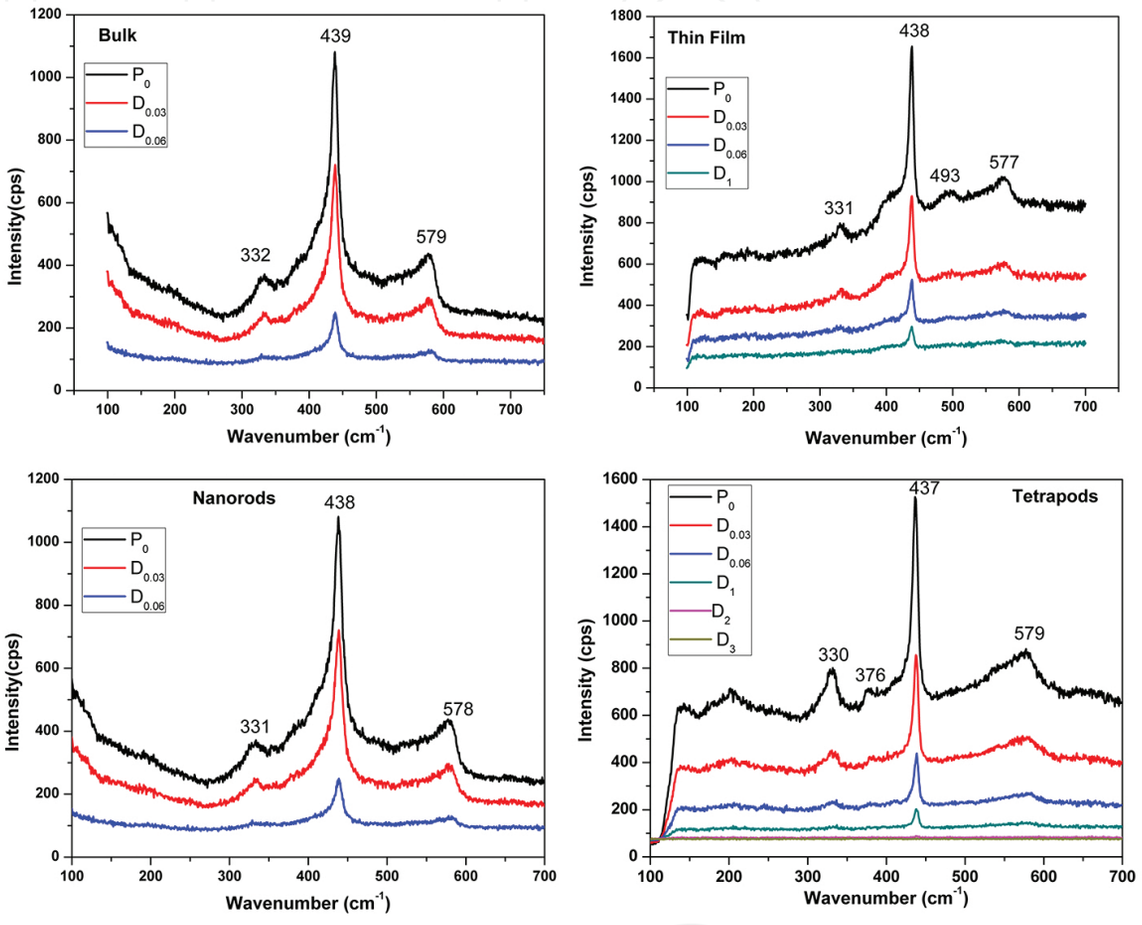

Figure 9. Raman spectrum of ZnO material for bulk, thin films, nanorods, and tetrapods.

Raman studies with 325 nm laser line are conducted on the ZnO nanostructures in order to cross check the laser heating effect because the same laser was used for the PL. The Raman spectra with 321 nm laser are shown in **Figure 10**. No E_2 (high) peak is observed. The LO mode is observed at 579/578/577 cm^{-1} for the different ZnO nanostructures. The intensity of LO is decreases with EI. Neither a blue nor a red shift is observed in LO position with a decrease in EI. According to previous report [13], the huge red shift of LO should be observed for the ZnO nanostructure when the intense local heating induced by UV laser. The observations from **Figure 10**, indirectly tells that the presence of the intrinsic impurity or defects in the sample. After careful analysis of Raman results, we understand that the huge shift of UV peak in PL may not be attributed to local heating induced by UV laser in the ZnO nanostructures. In order to verify this assumption, we recorded the PL and Raman spectra at low temperature for all

the samples using WITec Alpha SNOM instrument with solid state lasers 355 and 532 nm, respectively. We change the instrument to avoid instrumental error. Here, the PL spectrum was recorded at the maximum and minimum of laser EI. The samples were tested in the temperature range of −190 to 30°C (83–303 K).

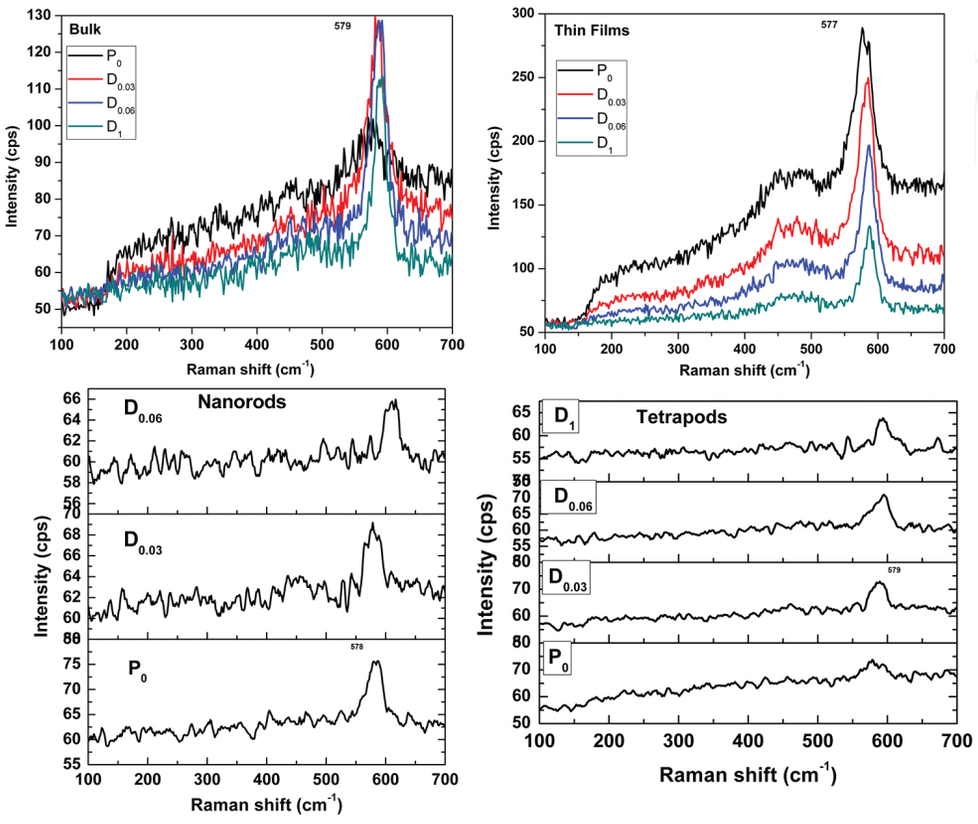

Figure 10. Raman spectrum of ZnO material with 325 nm excitation source for bulk, thin films, rods and tetrapods.

Figure 11 shows the low-temperature PL spectra. It is well known that the low-temperature PL from ZnO material with reasonably good crystalline quality is dominated by UV emission. From **Figure 11**, the origin of the UV emission peak shift explained based on the two major parameters one is laser EI the other one low-temperature variation.

From low-temperature PL, it can be argued that when the sample is in liquid nitrogen reservoir, then the reservoir temperature would be expected to compensate the local heating by laser. Hence, no-shift in the UV band (or the quenching of the UV emission) is expected. However, at liquid nitrogen temperature, the similar blue shift of UV emission has been observed for the samples (thin films, nanorods, and tetrapods) at *E*(max) and *E*(min). Moreover, we have tried to measure the surface temperature of the samples using thermocouple as well as IR thermometer during surface illumination by laser. No evidence of the increase in the surface temperature of the samples is observed. It is stated that such shift in UV emission is independent of the deposition parameter, morphology and structural parameters. The PL UV peak emission position blue shift of ZnO material can be understood from **Figure 12**.

http://dx.doi.org/10.5772/64937

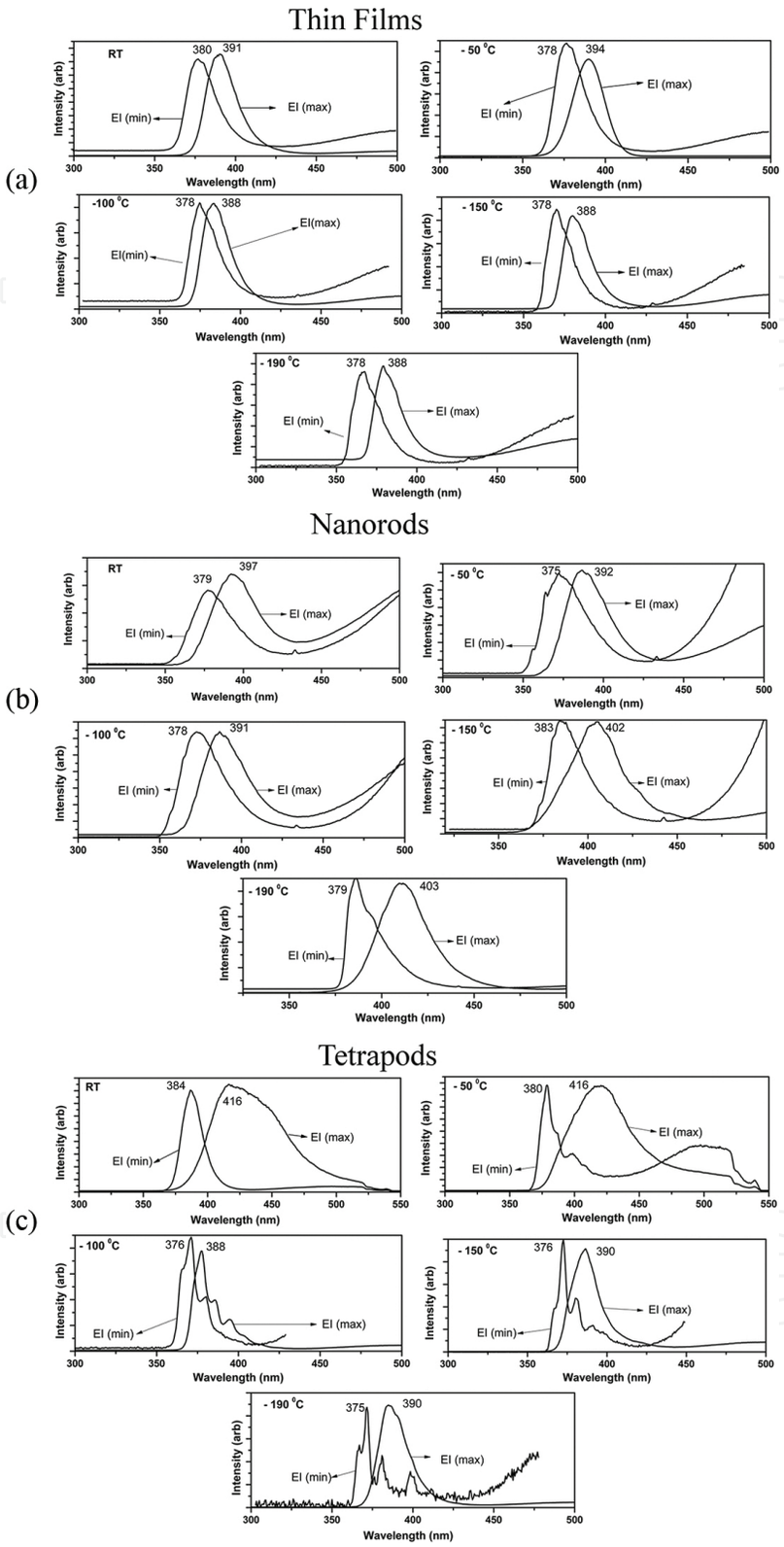

Figure 11. (a) Low-temperature PL of ZnO thin films. (b) Low-temperature PL of ZnO nanorod. (c) Low-temperature PL of ZnO tetrapods.

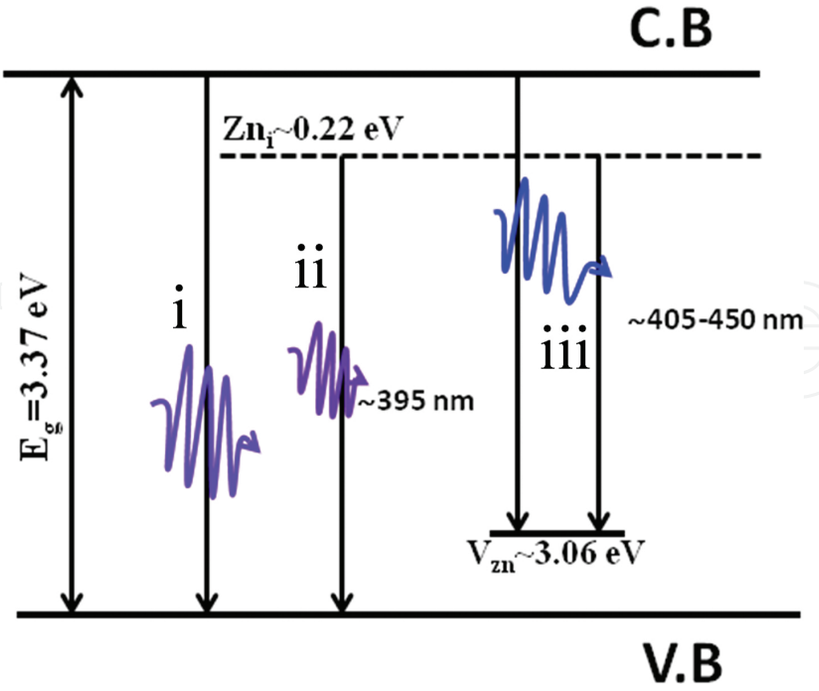

Figure 12. Energy band diagram of ZnO showing the probable transition processes [7].

After careful analysis of the RT and low-temperature PL studies, the shift in the UV emission can be due to intrinsic defect level emissions in ZnO as explained based on the energy band diagram shown in **Figure 12**. From **Figure 12**, the origin of UV emissions in ZnO are attributed to four factors. They are: (i) direct transition from conduction band (CB) to valence band (VB); (ii) transition of zinc interstitial (Zn_i) defect level to VB; (iii) transition from the CB to zinc vacancy (V_{Zn}) which is a result of blue-green emission of the material; and (iv) transition from Zn_i to V_{Zn} [7, 20]. It is believe that the Zn_i and V_{Zn} defects are playing crucial role in the blue shift of UV emission in ZnO. According to PL results, UV emission shifts largely from 377 to 415 nm with EIs for various samples. This UV emission can be due to the transitions (i), (ii), and (iii) involved between defects levels Zn_i, V_{Zn}, and CB due to which shift in the band-to-band transition is observed for different EIs. Hence, it is understood from the above discussion that defect levels present in the sample may be responsible for the shifts in the UV emission band with different EIs. In this regard, all ZnO samples exhibit the A_1LO Raman band (~580 cm^{-1}) which is ascribed to a defect induced mode [7] as evidenced from the Raman spectrum. Overall, all the samples possess considerable intrinsic defects which may be responsible for the shifts in UV emission band with EIs.

4. Conclusion

The excitation-intensity dependence of the UV emission for various ZnO samples has been studied in detail. The EI effects were studied systematically at room temperature and at liquid nitrogen temperature. It is observed that the UV emission band moves toward higher energy

side (blue shift) when the EI is decreased and vice versa both room temperature as well as at liquid nitrogen temperature. The blue shift of UV emission is only observed for some samples whereas few samples do show a marginal shift with the EI variation. These results give an implication that the shift may not be the intrinsic effect of laser-induced heating as has been claimed by other research groups; rather other mechanism can also be equally responsible. For detailed understanding, Raman measurements are methodically recorded for different EIs. The marginal shift in A_1LO modes observed for different samples with different EIs and systematic analysis of all the results supporting the shift of UV emission. It may also be attributed to the native defects in ZnO nanostructures/thin films apart from laser-induced heating. Result analysis show that the PL properties of the ZnO nanostructures/thin films are a strong function of the excitation intensity. The Raman studies helped to identify the origin of the UV emission peak shift in ZnO nanostructures. These results strongly suggest that heating effect alone cannot explain the observed excitation intensity dependency of luminescence spectra. However, further study is underway for better understanding.

Acknowledgements

The author is thankful to Dr K.K. Nanda, MRC, IISc, Dr G.K. Goswami, MRC, IISc, and Dr M.C. Santhosh Kumar, Department of Physics, NIT Tiruchirappalli for their help and discussion.

Author details

Prasada Rao Talakonda

Address all correspondence to: prasadview@gmail.com

Department of Physics, K L University, Andhra Pradesh, India

References

[1] S.S. Kurbanov, Kh.T. Igamberdiev, T.W. Kang. The UV-laser induced heating effect on photoluminescence from ZnO nanocrystals deposited on different substrates. J. Phys. D: Appl. Phys. 2010;43:115401. DOI:10.1088/0022-3727/43/11/115401.

[2] M. Kashif, S.M. Usman Ali, M.E. Ali, H.I. Abdulgafour, U. Hashim, M. Willander, Z. Hassan. Morphological, optical, and Raman characteristics of ZnO nanoflakes prepared via a sol–gel method. Phys. Status Solidi A, 2012;209:143–147. doi: 10.1002/pssa.201127357.

[3] Prasada Rao Talakonda, ZnO Thin films for Optoelectronic Applications, LAMBERT Academic Publishing, Heinrich-Bocking-Str. 6–8, 66121 Saarbrucken, Deutschland/ Germany, 2013, ISBN: 978-3-659-37010-6.

[4] J.C. Ronfard-Haret. Electric and luminescent properties of ZnO-based ceramics containing small amounts of Er and Mn oxide. J. Luminesc. 2003;104:1–12. doi:10.1016/S0022-2313(02)00574-4.

[5] Khedidja Bouzid, Abdelkader Djelloul, Noureddine Bouzid, Jamal Bougdira. Electrical resistivity and photoluminescence of zinc oxide films prepared by ultrasonic spray pyrolysis. Phys. Status Solidi A. 2009;206:106–115. doi: 10.1002/pssa.200824403.

[6] D.C. Reynolds, D.C. Look, B. Jogai, J.E. Van Nostrand, R. Jones, J. Jenny. Source of the yellow luminescence band in GaN grown by gas-source molecular beam epitaxy and the green luminescence band in single crystal ZnO. Solid State Commun. 1998;106:701–704. doi: 10.1016/S0038-1098(98)00048-9.

[7] T. Prasada Rao, G.K. Goswami, K.K. Nanda. Detailed understanding of the excitation-intensity dependent photoluminescence of ZnO materials: role of defects. J. Appl. Phys. 2014;115:213513. doi: 10.1063/1.4881779.

[8] Zhang YuGang, Zhang LiDe, Effect of excitation intensity on fluorescence spectra in ZnO nanostructures and its origin. Sci. China. Ser. G-Phys. Mech. Astron. 2009;52:4–12. doi: 10.1007/s11433-009-0008-2.

[9] T. Prasada Rao, M.C. Santhosh Kumar. Realization of stable p-type ZnO thin films using Li–N dual acceptors. J. Alloys Compd. 2011;509:8676–8682. doi:10.1016/j.jallcom.2011.05.094.

[10] S. Dhara, P.K. Giri. Rapid thermal annealing induced enhanced band-edge emission from ZnO nanowires, nanorods and nanoribbons. Funct. Mater. Lett. 2011;4:25–29. doi: 10.1142/S1793604711001658.

[11] Hongwei Yan, Yingling Yang, Zhengping Fu, Beifang Yang, Jian Zuo, Shengquan Fu. Excitation-power dependence of the near-band-edge photoluminescence of ZnO inverse opals and nanocrystal films. J. Luminesc. 2008;128:245–249. doi: 10.1016/j.jlumin.2007.08.002.

[12] E. Alarcon-Liado, J. Ibanez, R. Cusco, L. Artus, J.D. Prades, S. Estrade, J.R. Morante, Ultraviolet Raman scattering in ZnO nanowires:quasimodemixing and temperature effects. J. Raman Spectrosc. 2011;42:153–159. Doi: 10.1002/jrs.2664.

[13] K.A. Alim, V.A. Fonoberov, M. Shamsa, A.A. Balandin. Micro-Raman investigation of optical phonons in ZnO nanocrystals. J. Appl. Phys. 2005;97:124313. doi: 10.1063/1.1944222.

[14] R. Zhang, P.G. Yin, N. Wang, L. Guo. Photoluminescence and Raman scattering of ZnO nanorods. Solid State Sci. 2009;11:865–869. doi: 10.1016/j.solidstatesciences.2008.10.016.

[15] S.K. Panda, C. Jacob. Surface enhanced Raman scattering and photoluminescence properties of catalytic grown ZnO nanostructures. Appl. Phys A. 2009;96:805–811. doi: 10.1007/s00339-009-5309-9.

[16] I. Calizo, K.A. Alim, V.A. Fonoberov, S. Krishnakumar, M. Shamsa, A.A. Balandin, R. Kurtz. Micro-Raman spectroscopic characterization ZnO quantum dots, nanocrystals, and nanowires. Proc. SPIE. 2007;6481:64810N. doi: 10.1117/12.713648.

[17] K.A. Alim, V.A. Fonoberov, A.A. Balandin. Origin of the optical phonon frequency shifts in ZnO quantum dots. Appl. Phys. Lett. 2005;86:053103. doi: 10.1063/1.1861509.

[18] Y. Yang, H. Yan, Z. Fu, B. Yang, J. Zuo. Correlation between 577 cm^{-1} Raman scattering and green emission in ZnO ordered nanostructures. Appl. Phys. Lett. 2006;88:191909. doi: 10.1063/1.2202741.

[19] C. Xu, G. Xu, Y. Liu, G. Wang. A simple and novel route for the preparation of ZnO nanorods. Solid. State. Commun. 2000;122:175–179. doi:10.1016/S0038-1098(02)00114-X.

[20] A.N. Mallika, A. Ramachandra Reddy, K. Sowribabu, K. Venugopal Reddy. Structural and optical characterization of $Zn_{0.95-x}Mg_{0.05}Al_xO$ nanoparticles. Ceram. Int. 2015;41:9276–9284. doi:10.1016/j.ceramint.2015.03.096.

IntechOpen